

Synthesis and Electropolymerization of 1,4-Bis(2-Thienyl)-2,5-Difluorobenzene and its Electrochromic Properties and Electrochromic Device Application

Bin Wang¹, Tianyu Kong², Jinsheng Zhao^{1,*}, Chuansheng Cui¹, Renmin Liu¹, Qingpeng He¹

¹ Shandong Key Laboratory of Chemical Energy-storage and Novel Cell Technology, Liaocheng University, 252059, Liaocheng, P. R. China.

² State key Laboratory of Electronic Thin Films and Integrated Devices(UESTC)

*E-mail: j.s.zhao@163.com

Received: 22 November 2011 / Accepted: 17 December 2011 / Published: 1 January 2012

1,4-Bis(2-thienyl)-2,5-difluorobenzene monomer was successfully synthesized via Suzuki coupling reaction. Poly(1,4-bis(2-thienyl)-2,5-difluorobenzene) (PTF₂P) was electrochemically synthesized and characterized. Characterizations of the resulting polymer PTF₂P were performed by cyclic voltammetry (CV), UV-vis spectroscopy, Fourier transform infrared spectroscopy (FT-IR) and scanning electron microscopy (SEM). Moreover, the spectroelectrochemical and electrochromic properties of the polymer film were investigated. The resulting polymer film has distinct electrochromic properties and shows five different colors (yellow, yellowish green, green, greenish blue and blue) under various potentials. The PTF₂P film shows a maximum optical contrast ($\Delta T\%$) of 46% at 605 nm with a response time of 1.92 s. The coloration efficiency (CE) of PTF₂P film was calculated to be 178.8 cm² C⁻¹. An electrochromic device (ECD) based on PTF₂P and poly(3,4-ethylenedioxythiophene) (PEDOT) was also constructed and characterized. The optical contrast ($\Delta T\%$) at 630 nm was found to be 27% and response time was measured as 0.66 s. The CE of the device was calculated to be 491.4 cm² C⁻¹. This ECD has satisfactory redox stability.

Keywords: Conjugated polymer; Spectroelectrochemistry; Electrochemical polymerization; Electrochromic device; 1,4-Bis(2-thienyl)-2,5-difluorobenzene.

1. INTRODUCTION

Conducting polymers continue to receive much attention because of their ease of synthetic accessibility and perfectly controlled architecture that allows a fine-tuning of the intrinsic properties, e.g. electronic, optical, conductivity, etc. [1]. These polymers are excellent candidates for applications

in displays [2], light emitting diodes [3], photovoltaic devices [4] and electrochromic devices [5,6]. For electrochromic device applications, electrochromism is the reversible change in optical properties that can occur when a material is electrochemically oxidized (loss of electron(s)) or reduced (gain of electron(s)) [7]. Conjugated polymers (CPs) stand for a family of important electrochromic materials that have recently received much attention due to their several advantages over inorganic compounds. These include outstanding coloration efficiency, fast switching ability, multiple colors with the same material and fine-tunability of the band gap (and the color), excellent processability and low cost [8]. To achieve color change in electrochromic polymers, absorption in the visible region should be monitored by means of an externally applied potential. Upon doping, electronic states change due to the formation of polaronic and bipolaronic bands causing a change in the absorption characteristics of the polymer [2,9].

Among the electrochromic conjugated polymers, polythiophenes have occupied prime position due to its high conductivity, good redox reversibility, swift change of color with potential, and stability in environment [10]. Synthesis of new polythiophene derivatives with the ability to tailor the electrochromic properties is an important part of conducting polymer research [11,12]. Structural modification of conjugated polymer chains has proved useful in the preparation of redox dopable electronically conducting polymers with a broad range of mechanical, electrical, electrochemical and optical properties [13]. Now, a series of phenylene-substituted di-2-thienylphenylene polymers have been synthesized, these polymers demonstrate electrochemical and optical properties very similar to polythiophene, while retaining the synthetic flexibility for substitution found in phenylenes [13]. Among these polymers, a family of polymers containing alternating thiophene and fluorine-substituted phenylene units has been synthesized and characterized [14–16]. The introduction of fluorine on the polymer backbone can stabilize the excess negative charge in the n-doped state increasing the doping level and stability of the polymer [15]. The synthesis and characterization of 1,4-bis(2-thienyl)-2,5-difluorobenzene has been reported by J.R. Reynolds [16]. However, to the best of our knowledge, there are still no reports on the electrochromic devices of poly(1,4-bis(2-thienyl)-2,5-difluorobenzene).

According to above consideration, in this study, 1,4-bis(2-thienyl)-2,5-difluorobenzene (TF₂P) monomer was synthesized via Suzuki coupling reaction. Electrochemical polymerization of TF₂P monomer is successfully carried out in 0.2 M NaClO₄/acetonitrile (ACN) solution. The spectroelectrochemical and electrochromic properties of the PTF₂P film are investigated in detail. The PTF₂P film shows yellow color at neutral state and blue color at full doped state. In addition, we constructed and characterized dual type electrochromic devices based on PTF₂P and PEDOT in detail. Neutral state of device shows yellowish green color, while oxidized state reveals blue color.

2. EXPERIMENTAL

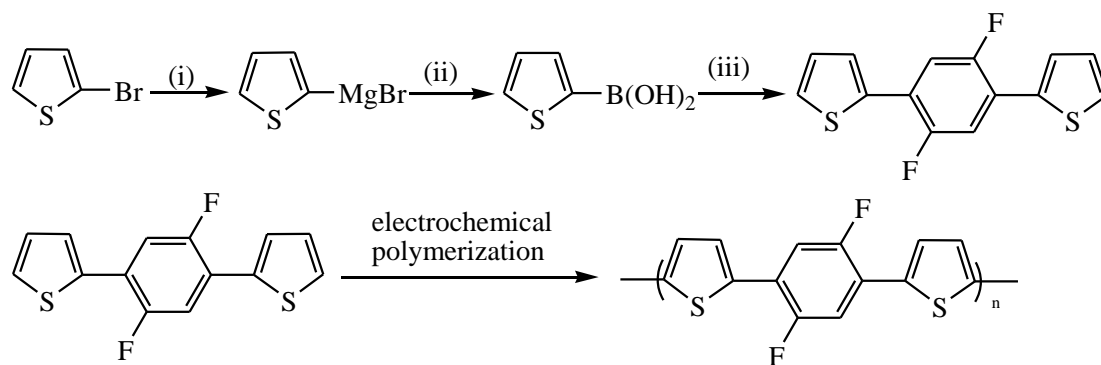
2.1. Materials

1,4-Dibromo-2,5-difluorobenzene, 2-bromothiophene, trimethylborate (B(OMe)₃), tetrakis(triphenylphosphine)palladium(0) (Pd(PPh₃)₄) and 3,4-ethylenedioxythiophene (EDOT, 98%)

were purchased from Aldrich Chemical and used as received. Commercial high-performance liquid chromatography grade acetonitrile (ACN, Tedia Company, INC., USA), poly(methyl methacrylate) (PMMA, Shanghai Chemical Reagent Company), propylene carbonate (PC, Shanghai Chemical Reagent Company) and lithium perchlorate (LiClO_4 , Shanghai Chemical Reagent Company, 99.9%) were used directly without further purification. Sodium perchlorate (NaClO_4 , Shanghai Chemical Reagent Company, 98%) was dried in vacuum at 60 °C for 24 h before use. Other reagents were all used as received without further treatment. Indium-tin-oxide-coated (ITO) glass (sheet resistance : < 10 $\Omega \square^{-1}$, purchased from Shenzhen CSG Display Technologies, China) was washed with ethanol, acetone and deionized water successively under ultrasonic, and then dried by N_2 flow.

2.2. Synthesis of 1,4-bis(2-thienyl)-2,5-difluorobenzene (TF_2P)

1,4-Bis(2-thienyl)-2,5-difluorobenzene (TF_2P) was synthesized via Suzuki coupling reaction. As shown in Scheme 1, 2-bromothiophene in a dry ethylether (Et_2O) was added dropwise to a stirred suspension of magnesium powder in anhydrous Et_2O at room temperature. The obtained Grignard reagent was reacted with trimethylborate ($\text{B}(\text{OMe})_3$) in dry tetrahydrofuran (THF) to afford (2-thienyl)boronic acid, which was then cross-coupled to 1,4-dibromo-2,5-difluorobenzene in the presence of catalytic tetrakis(triphenylphosphine)palladium(0) ($\text{Pd}(\text{PPh}_3)_4$). The purified product was a white solid. ^1H NMR and FT-IR spectra verified the structure and purity of the TF_2P monomer.



Scheme 1. Synthetic routes of monomer and polymer. Reagents: (i) Mg, Et_2O ; (ii) $\text{B}(\text{OMe})_3$, THF; (iii) 1,4-dibromo-2,5-difluorobenzene, $\text{Pd}(\text{PPh}_3)_4$, THF.

2.3. Instrumentation

^1H NMR spectroscopy studies were carried out on a Varian AMX 400 spectrometer and tetramethylsilane (TMS) was used as the internal standard for ^1H NMR. FT-IR spectra were recorded on a Nicolet 5700 FT-IR spectrometer, where the samples were dispersed in KBr pellets. Scanning electron microscopy (SEM) measurements were taken using a Hitachi SU-70 thermionic field emission SEM. UV-vis spectra were carried out on a Perkin-Elmer Lambda 900 UV-vis-near-infrared

spectrophotometer. Digital photographs of the polymer films and device cell were taken by a Canon Power Shot A3000 IS digital camera.

2.4. Electrochemistry

Electrochemical synthesis and experiments were performed in a one-compartment cell with a CHI 760 C Electrochemical Analyzer under computer control, employing a platinum wire with a diameter of 0.5 mm as the working electrode, a platinum ring as the counter electrode, and a silver wire (Ag wire) as the pseudo reference electrode. The working and counter electrodes for cyclic voltammetric (CV) experiments were placed 0.5 cm apart during the experiments. All electrochemical polymerization and CV tests were taken in ACN solution containing 0.2 M NaClO₄ as the supporting electrolyte. The pseudo reference electrode was calibrated externally using a 5 mM solution of ferrocene (Fc/Fc⁺) in the electrolyte ($E_{1/2}(\text{Fc}/\text{Fc}^+) = 0.20 \text{ V vs. Ag wire in } 0.2 \text{ M NaClO}_4/\text{ACN}$) [17]. The half-wave potential ($E_{1/2}$) of Fc/Fc⁺ measured in 0.2 M NaClO₄/ACN solution is 0.28 V vs. SCE. Thus, the potential of Ag wire was assumed to be 0.08 V vs. SCE [18]. All of the electrochemical experiments were carried out at room temperature under nitrogen atmosphere.

2.5. Spectroelectrochemistry

Spectroelectrochemical data were recorded on Perkin-Elmer Lambda 900 UV–vis–near-infrared spectrophotometer connected to a computer. A three-electrode cell assembly was used where the working electrode is an ITO glass, the counter electrode was a stainless steel wire, and an Ag wire was used as the pseudo reference electrode. The polymer films for spectroelectrochemistry were prepared by potentiostatically deposition on ITO electrode (the active area: 0.8 cm × 2.0 cm). The measurements were carried out in 0.2 M NaClO₄/ACN solution.

2.6. Preparation of the gel electrolyte

A gel electrolyte based on PMMA and LiClO₄ was plasticized with PC to form a highly transparent and conductive gel. ACN was also included as a high vapor pressure solvent to allow an easy mixing of the gel components. The composition of the casting solution by weight ratio of ACN:PC:PMMA:LiClO₄ was 70:20:7:3. The gel electrolyte was used for construction of the polymer electrochromic device cell [19].

2.7. Construction of ECDs

ECDs were constructed using two complementary polymers, namely PTF₂P as the anodically coloring material and PEDOT as the cathodically coloring material. The PTF₂P and PEDOT films were electrodeposited on two ITO glasses (the active area: 1.8 cm × 2.5 cm) at 1.4 V. Electrochromic

device was built by arranging the two polymer films (one oxidized, the other reduced) facing each other separated by a gel electrolyte.

3. RESULTS AND DISCUSSION

3.1. ^1H NMR spectrum, FTIR spectra of TF_2P monomer

^1H NMR spectrum of TF_2P (Fig. 1): $\text{C}_{14}\text{H}_8\text{S}_2\text{F}_2$, δ_{H} (ppm, CDCl_3): 7.513 (d, 2H), 7.432–7.387 (m, 4H), 7.135 (t, 2H). The 5-thienyl proton resonance was observed as a doublet at 7.513 ppm, while the 4-thienyl proton was found as a triplet at 7.135 ppm. The 3-thienyl and the phenyl protons overlap in the 7.432–7.387 ppm range [16].

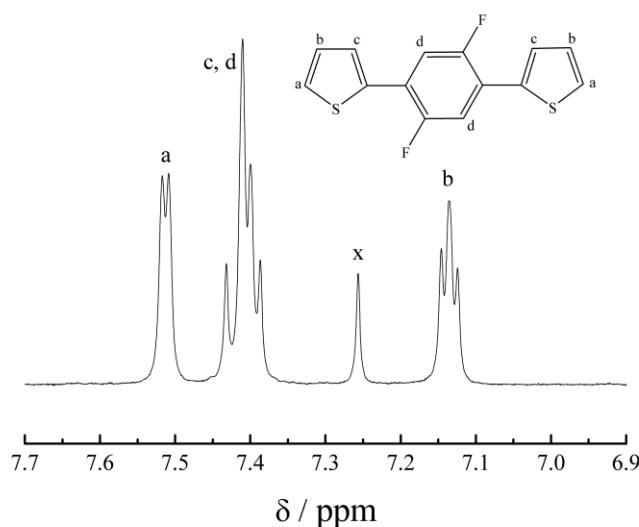


Figure 1. ^1H NMR spectrum of 1,4-bis(2-thienyl)-2,5-difluorobenzene (TF_2P) monomer in CDCl_3 . Solvent peak at $\delta = 7.257$ ppm is marked by 'x'.

FT-IR spectrum of TF_2P monomer is shown in Fig. 4a. In the spectrum of TF_2P , the band around 1539 cm^{-1} is ascribed to the stretching vibrations of phenylene rings, and the bands at 1487 and 1437 cm^{-1} are due to the stretching vibrations of thiophene rings [13]. The C-H_β and C-H_α out-of-plane bending of thiophene are observed at 818 and 688 cm^{-1} , respectively [20].

3.2. Electrochemical polymerization and characterization of PTF_2P films

3.2.1. Electrochemical polymerization

The successive CV curves of 0.005 M TF_2P in 0.2 M $\text{NaClO}_4/\text{ACN}$ are illustrated in Fig. 2. The onset oxidation potential (E_{onset}) of TF_2P in the solution is 1.25 V , which is higher than that of 1,4-

bis(2-thienyl)-benzene monomer (1.05 V) in the same electrolyte solution [18]. This phenomenon arises because the excess charge of the radical cation is delocalized over the aromatic backbone and the increase in electron withdrawing character of the phenylene group due to the introduction of fluorine atoms [21].

As the CV scan continued, PTF₂P film was formed on the working electrode surface. The increases in the redox wave current densities imply that the amount of conducting polymers deposited on the electrode were increasing [22]. The CV curves of TF₂P show distinct reduction waves at 1.07 V, while the corresponding oxidation waves are overlapped with the oxidation waves of the TF₂P monomer and cannot be observed clearly [23].

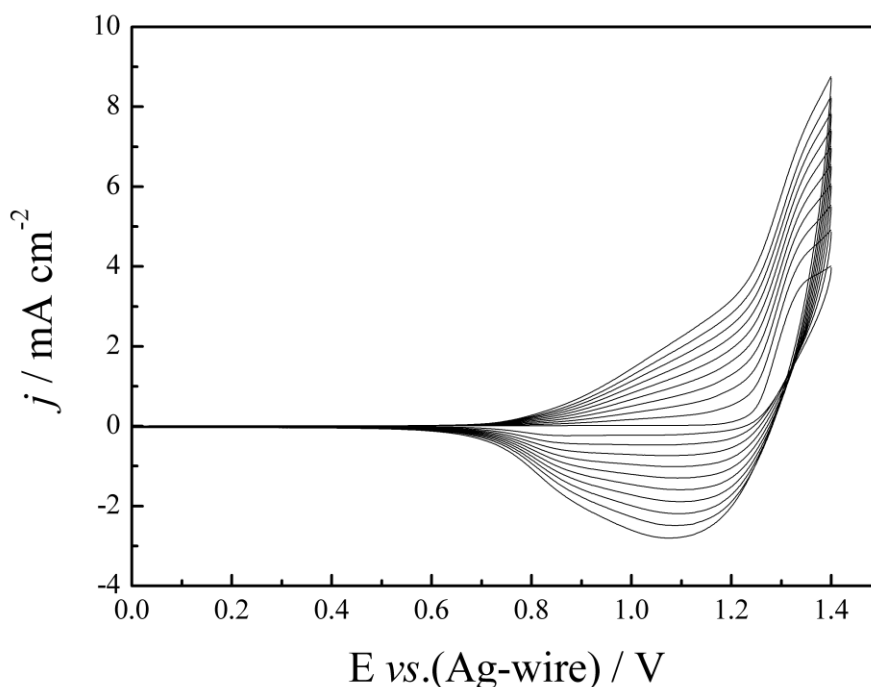


Figure 2. Cyclic voltammogram curves of 0.005 M TF₂P in 0.2 M NaClO₄/ACN solution at a scan rate of 100 mV s⁻¹, j denotes the current density.

3.2.2. Electrochemistry of the PTF₂P film

Fig. 3 shows the electrochemical behavior of the PTF₂P film (prepared on platinum wires by sweeping the potentials from 0 to 1.4 V for three cycles) at different scan rates between 25 and 300 mV s⁻¹ in 0.2 M NaClO₄/ACN.

As shown in Fig. 3, the peak current density (j) response increases with the increasing of the scan rate, indicating that the polymer film adheres well to the electrode [23]. However, the scan rate dependence of the current densities response of PTF₂P is not linear, thus the polymer is only poorly electroactive [16].

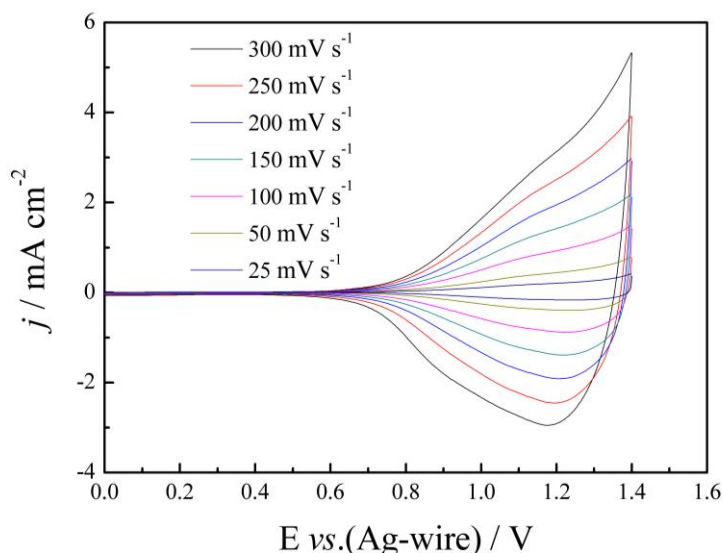


Figure 3. CV curves of the PTF₂P film at different scan rates between 25 and 300 mV s⁻¹ in a monomer-free 0.2 M NaClO₄/ACN solution, *j* denotes the current density.

3.2.3. FT-IR spectrum of PTF₂P

To obtain a sufficient amount of PTF₂P film for characterization, the ITO glass (the active area: 1.8 cm × 2.5 cm) was employed as the working electrode. The polymer was synthesized at 1.4 V vs. Ag wire potentiostatically in a solution of 0.2 M NaClO₄/ACN containing 0.005 M TF₂P. Fig. 4b shows the FT-IR spectrum of PTF₂P. The absorption peak at 785 cm⁻¹ is due to the out-of-plane bending vibrations of C–H bonding in β-position of the 2,5-disubstituted thiophene rings [24]. Compare to the spectrum of TF₂P, the disappearance of the C–H_α out-of-plane bending vibrations of thiophene at 688 cm⁻¹ implies that the polymerization occurs at the α-position of thiophene rings.

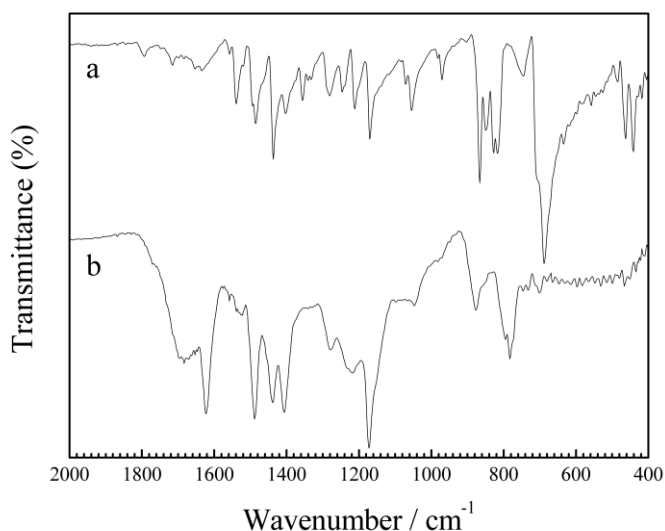


Figure 4. The FT-IR spectra of (a) TF₂P monomer and (b) PTF₂P prepared potentiostatically at 1.4 V.

3.2.4. Morphology

The morphology of PTF₂P film was investigated by scanning electron microscopy (SEM). The PTF₂P film was prepared by constant potential electrolysis from the solution of 0.2 M NaClO₄/ACN containing 0.005 M monomer on ITO electrode and dedoped before characterization. As shown in Fig. 5, the PTF₂P film exhibits an accumulation state of clusters of globules. Compare to the morphology of poly(1,4-bis(2-thienyl)-benzene) [18], the PTF₂P film shows porous structure.

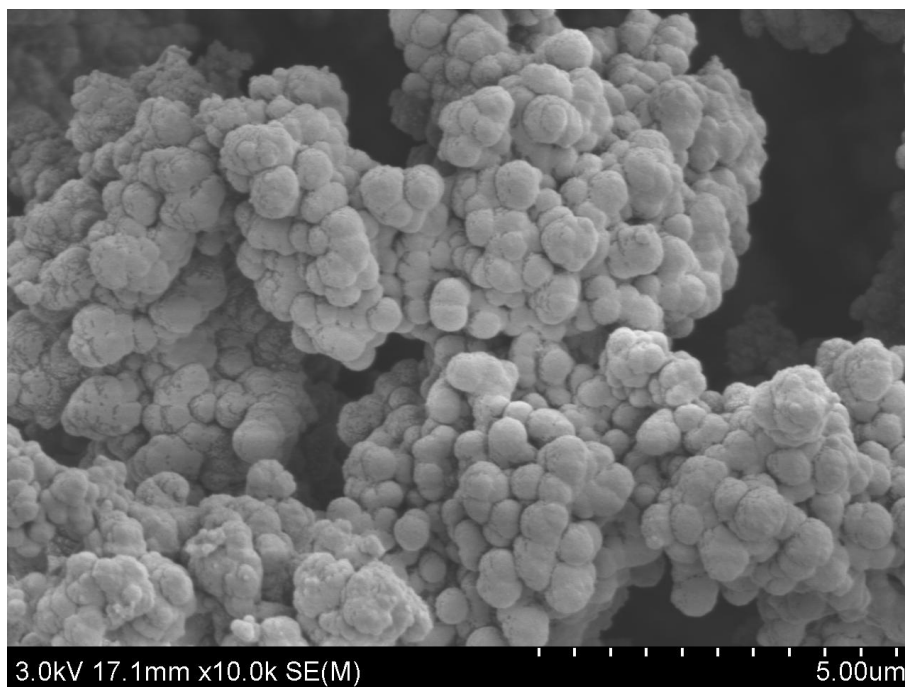


Figure 5. SEM images of PTF₂P deposited on ITO electrode potentiostatically at 1.4 V.

3.2.5. Optical properties of TF₂P monomer and PTF₂P film

The UV–vis spectra of TF₂P monomer in CH₂Cl₂ and PTF₂P film deposited on ITO electrode are shown in Fig. 6. As seen from Fig. 6, the absorption maximum (λ_{\max}) of the monomer TF₂P and the neutral state PTF₂P are centered at 335 and 410 nm, respectively. The difference between the λ_{\max} corresponding to the monomer and the corresponding polymer for TF₂P; 75 nm is owing to the increased conjugation length in the polymer [25]. The λ_{\max} of TF₂P monomer exhibits a 11 nm red shift compare to that of 1,4-bis(2-thienyl)-benzene (BTB, 324 nm) [18].

In addition, the optical band gap (E_g) of polymer was calculated from its low energy absorption edges (λ_{onset}) ($E_g = 1241/\lambda_{\text{onset}}$) [26]. The E_g of the PTF₂P film was calculated as 2.32 eV, which is only 0.01 eV higher than that of poly(1,4-bis(2-thienyl)-benzene) (PBTB) film (2.31 eV) [18]. Table 1 summarizes the onset oxidation potential (E_{onset}), maximum absorption wavelength (λ_{\max}) and the optical band gap (E_g) of the TF₂P, BTB, PTF₂P and PBTB quite clearly. HOMO energy levels of them were calculated by using the formula $E_{\text{HOMO}} = -e(E_{\text{onset}} + 4.4)$ (E_{onset} vs. SCE) and LUMO energy

levels (E_{LUMO}) of them were calculated by the subtraction of the optical band gap from the HOMO levels [27,28].

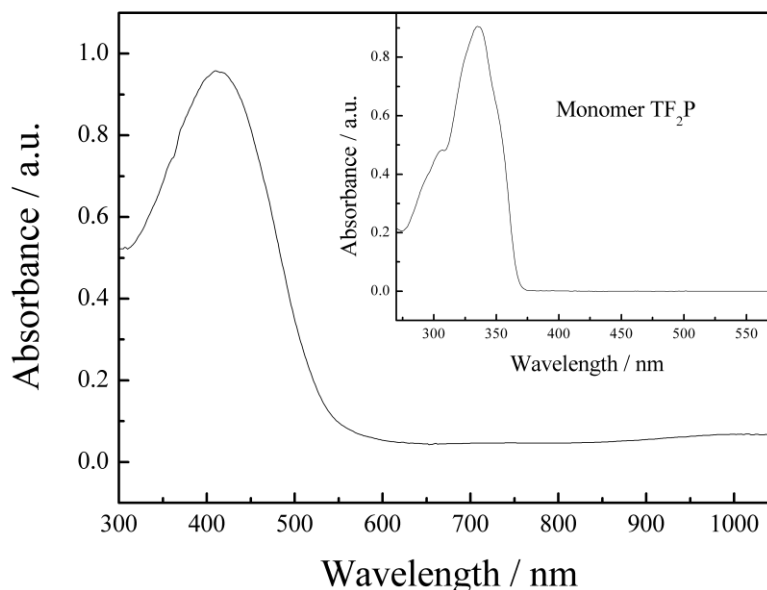


Figure 6. UV-vis spectrum of PTF₂P film deposited on ITO electrode at the neutral state. Inset: absorption spectrum of TF₂P monomer dissolved in CH₂Cl₂.

Table 1. The onset oxidation potential (E_{onset}), maximum absorption wavelength (λ_{max}), HOMO and LUMO energy levels and optical band gap (E_{g}) of TF₂P, BTB, PTF₂P and PBTB.

Compounds	E_{onset} , vs.(Ag-wire) (V)	λ_{max} (nm)	E_{g} (eV)	HOMO (eV)	LUMO ^a (eV)
TF ₂ P	1.25	335	3.38	-5.73	-2.35
BTB ^b	1.05	324	3.41	-5.53	-2.12
PTF ₂ P	0.80	410	2.32	-5.28	-2.96
PBTB ^b	0.72	411	2.31	-5.20	-2.89

^a Calculated by the subtraction of the optical band gap from the HOMO level.

^b Data were taken from Ref. [18].

3.3. Electrochromic properties of PTF₂P film

3.3.1. Spectroelectrochemical properties of PTF₂P film

Spectroelectrochemistry is a useful method for studying the changes in the absorption spectra and the information about the electronic structures of conjugated polymers as a function of the applied potential difference [29]. The PTF₂P film (coated on ITO, prepared potentiostatically at 1.4 V in 0.2 M NaClO₄/ACN solution mixing with 0.005 M TF₂P monomer) was switched between 0 and 1.35 V in a monomer-free 0.2 M NaClO₄/ACN solution in order to obtain the in situ UV-vis spectra (Fig. 7). At

the neutral state, the polymer film exhibits an absorption band at 411 nm due to the π - π^* transition. As shown in Fig. 7, the intensity of the PTF₂P π - π^* electron transition absorption decreases while two charge carrier absorption bands located at around 605 nm and longer than 1050 nm increase dramatically upon oxidation. The appearance of charge carrier bands could be attributed to the evolution of polaron and bipolaron bands.

Furthermore, the PTF₂P film shows five colors under various potentials. At 0 V, the film shows a yellow color which passes to a yellowish green at 1.00 V. With the increase of potential, the polymer film turns into green (1.15 V), greenish blue (1.20 V) and eventually to a blue color at 1.30 V, respectively (Fig. 8). Compare to PBTB film, the full doped state PTF₂P film shows a blue color while PBTB film reveals green color at full doped state.

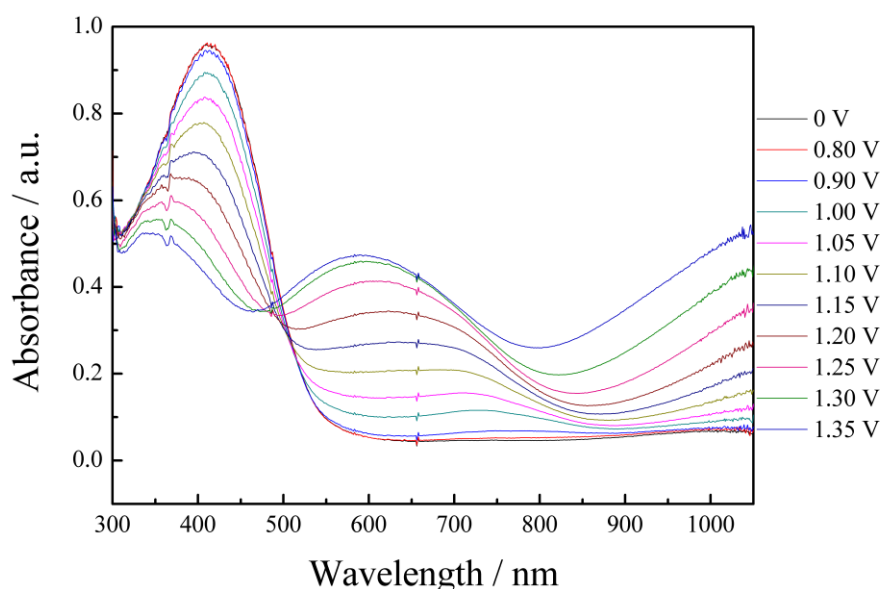


Figure 7. Spectroelectrochemical spectra of PTF₂P film on ITO electrode with applied potentials between 0 V and 1.35 V in monomer-free 0.2 M NaClO₄/ACN solution.

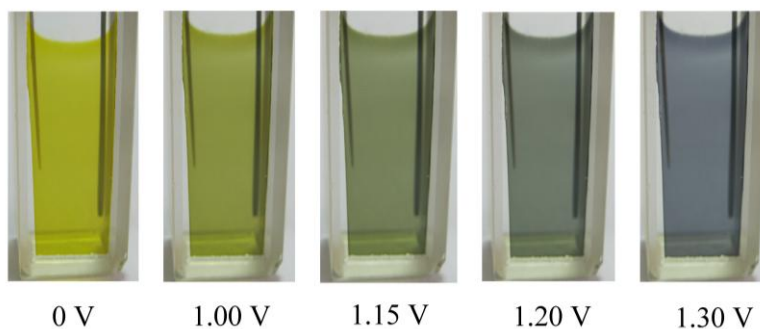


Figure 8. Multichromic behavior of PTF₂P film at 0 V (yellow), 1.00 V (yellowish green), 1.15 V (green), 1.20 V (greenish blue) and 1.30 V (blue).

3.3.2. Electrochromic switching of PTF₂P film in solution

It is important that polymers can switch rapidly and exhibit a noteworthy color change for electrochromic applications [30]. For this purpose, double potential step chronoamperometry technique was used to investigate the switching ability of PTF₂P film between its neutral and full doped states (Fig. 9) [31]. The dynamic electrochromic experiment for PTF₂P film was carried out at 605 nm. The potential was switched between 0 V (the neutral state) and 1.35 V (the oxidized state) with regular intervals of 3 s. One important characteristic of electrochromic materials is the optical contrast ($\Delta T\%$), which can be defined as the transmittance difference between the redox states. The $\Delta T\%$ of the PTF₂P was found to be 46% at 605 nm as shown in Fig. 9.

Response time, one of the most important characteristics of electrochromic materials, is the necessary time for 95% of the full optical switch (after which the naked eye could not sense the color change) [32]. The optical response time of PTF₂P was found to be 1.92 s from the reduced to the oxidized state and 0.38 s from the oxidized to the reduced state at 605 nm. The PTF₂P film has similar optical contrast and slower response time compare to PBTB [18].

The coloration efficiency (CE) is also an important characteristic for the electrochromic materials. CE can be calculated by using the equations and given below [33]:

$$\Delta OD = \lg\left(\frac{T_b}{T_c}\right) \quad \text{and} \quad \eta = \frac{\Delta OD}{\Delta Q}$$

where T_b and T_c are the transmittances before and after coloration, respectively. ΔOD is the change of the optical density, which is proportional to the amount of created color centers. η denotes the coloration efficiency (CE). ΔQ is the amount of injected charge per unit sample area. CE of PTF₂P film is measured as 178.8 cm² C⁻¹ (at 605 nm) at full doped state, which had reasonable coloration efficiency.

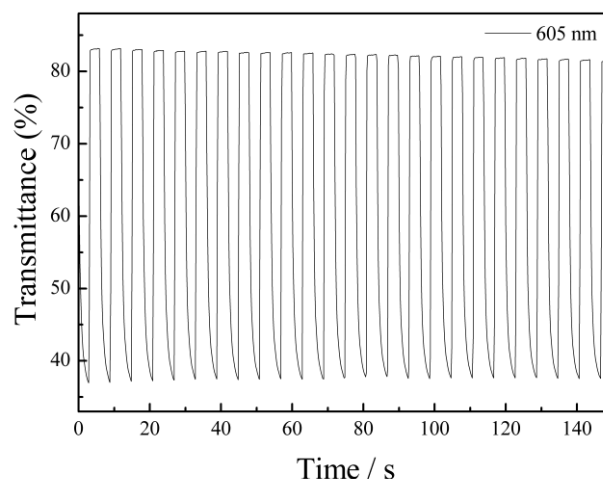


Figure 9. Electrochromic switching response for PTF₂P film monitored at 605 nm in 0.2 M NaClO₄/ACN solution between 0 V and 1.35 V with a residence time of 3 s.

3.4. Spectroelectrochemistry of electrochromic devices (ECDs)

3.4.1. Spectroelectrochemical properties of ECD

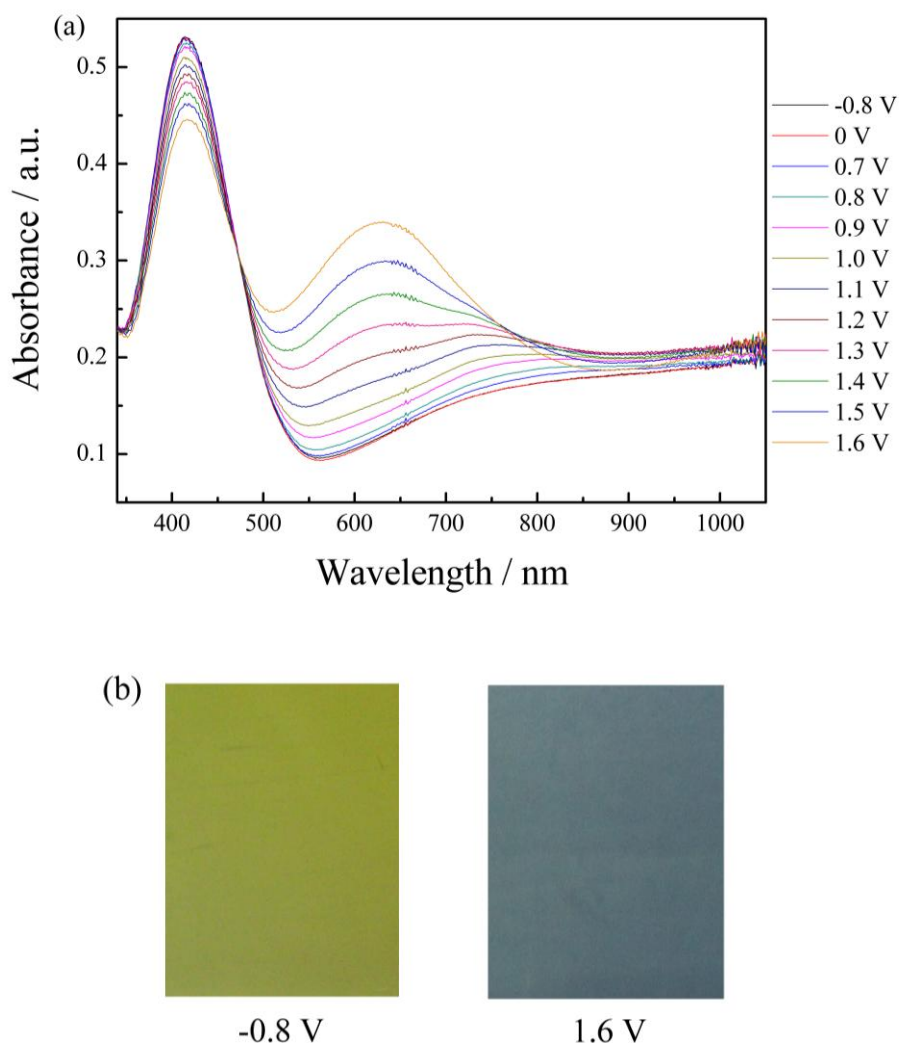


Figure 10. (a) Spectroelectrochemical spectra of the PTF₂P/PEDOT device at various applied potentials from -0.8 to 1.6 V and (b) the colors of the device at -0.8 V (the neutral state) and 1.6 V (the oxidized state).

A dual type ECD consisting of PTF₂P and PEDOT was constructed and its spectroelectrochemical behaviors were studied. Before composing the ECD, the anodically coloring polymer film PTF₂P was fully reduced and the cathodically coloring polymer PEDOT was fully oxidized. The spectroelectrochemical spectra of the PTF₂P/PEDOT device as a function of applied potential (between -0.8 V and 1.6 V) are given in Fig. 10. The PTF₂P layer is in its neutral state at -0.8 V, where the absorption at 414 nm is due to π - π^* transition of the PTF₂P film. At that state, PEDOT does not reveal an obvious absorption at the UV-vis region of the spectrum and device reveals

yellowish green color. As the applied potential increases, the PTF₂P layer starts to get oxidized and the intensity of the peak due to the π - π^* transition decreased. Meanwhile, PEDOT layer is in its reduced state, which leads to a new absorption at 630 nm due to the reduction of PEDOT, and the dominated color of the device is blue at 1.6 V (Fig. 10).

3.4.2. Switching of ECD

Kinetic studies were also done to test the response time of PTF₂P/PEDOT ECD. Between -0.8 and 1.6 V inputs with a regular time interval of 2 s, the optical response at 630 nm was illustrated in Fig. 11. The response time was found to be 0.66 s at 95% of the maximum transmittance difference from the neutral state to oxidized state and 0.20 s from the oxidized state to the neutral state, and optical contrast ($\Delta T\%$) was calculated to be 27% . The PTF₂P/PEDOT device has similar response time and optical contrast compared with the PBTB/PEDOT device [18]. The CE of the device (the active of area: 1.8 cm \times 2.0 cm) was calculated to be 491.4 cm² C⁻¹ at 630 nm.

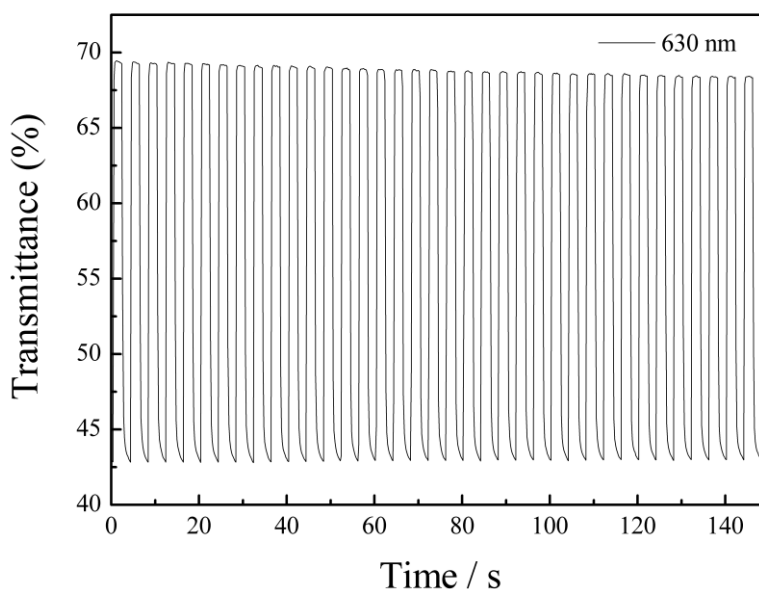


Figure 11. Electrochromic switching, optical transmittance change monitored at 630 nm for PTF₂P/PEDOT device between -0.8 V and 1.6 V with a residence time of 2 s.

3.4.3. Open circuit memory of ECD

The optical memory in the electrochromic devices is an important parameter because it is directly related to its application and energy consumption during the use of ECDs [34]. The optical spectrum for PTF₂P/PEDOT device was monitored at 630 nm as a function of time at -0.8 V and 1.6 V by applying the potential for 1 s for 200 and 100 s time intervals, respectively. As shown in Fig. 12, at yellowish green colored state device shows a true permanent memory effect since there is almost no transmittance change under applied potential or open circuit conditions. In blue colored state device is

rather less stable in terms of color persistence, however this matter can be overcome by application of current pulses to freshen the fully colored states.

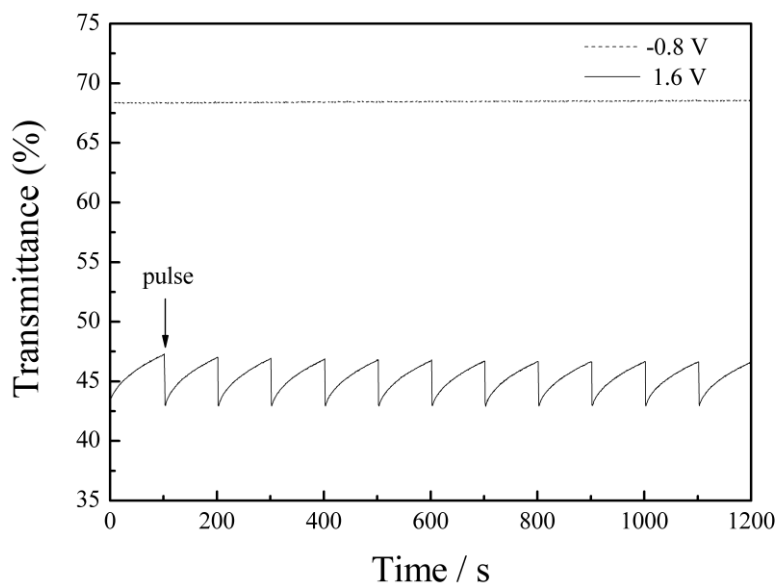


Figure 12. Open circuit stability of the PTF₂P/PEDOT device monitored at 630 nm.

3.4.4. Stability of ECD

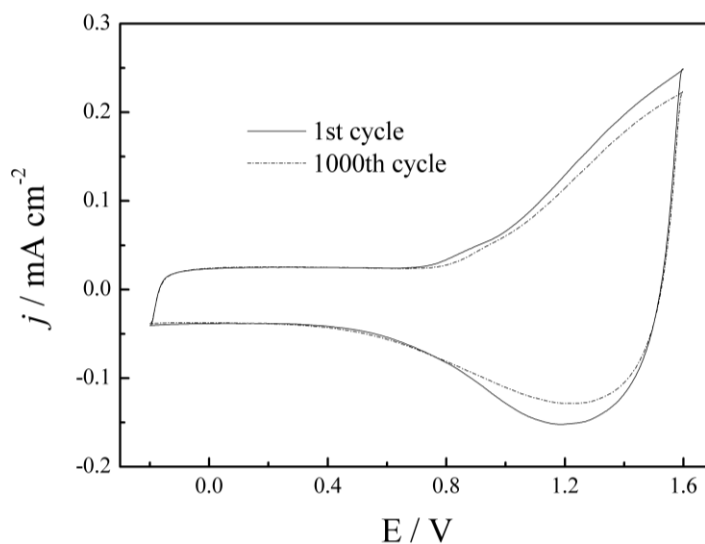


Figure 13. Cyclic voltammogram of PTF₂P/PEDOT device as a function of repeated with a scan rate of 500 mV s⁻¹.

The stability of the devices toward multiple redox switching usually limits the utility of electrochromic materials in ECD applications. Therefore, redox stability is another important

parameter for ECD [35]. For this reason, the PTF₂P/PEDOT device was tested with cyclic voltammetry by applying potentials between -0.2 and 1.6 V with 500 mV s⁻¹ to evaluate the stability of the device (Fig. 13). After 1000 cycles, the CV curve reveals the device retaining 92% of its original electroactivity, which indicating that this device has satisfactory redox stability.

4. CONCLUSIONS

1,4-Bis(2-thienyl)-2,5-difluorobenzene monomer was synthesized by Suzuki coupling reaction and then its polymer was successfully synthesized by electrochemical oxidation of the monomer in 0.2 M NaClO₄/ACN solution. The obtained polymer film was studied by cyclic voltammetry, UV-vis spectra, FT-IR spectra and scanning electron microscopy. Spectroelectrochemistry reveals that PTF₂P film has distinct electrochromic properties and shows five different colors under various potentials (yellow, yellowish green, green, greenish blue and blue). Maximum contrast ($\Delta T\%$) and response time of the PTF₂P film were measured as 46% and 1.92 s at 605 nm. The dual type ECD based on PTF₂P and PEDOT was also constructed and characterized. Electrochromic switching study results show that optical contrast ($\Delta T\%$) and response time were 27% and 0.66 s at 630 nm, respectively. The CE of the ECD was calculated to be 491.4 cm² C⁻¹. This ECD shows yellowish green color at neutral state and blue color at oxide state.

ACKNOWLEDGEMENTS

The work was financially support by the National Natural Science Foundation of China (20906043), the Promotive research fund for young and middle-aged scientists of Shandong Province (2009BSB01453), the Natural Science Foundation of Shandong province (ZR2010BQ009), the open foundation of the State key Laboratory of Electronic Thin Films and Integrated Devices(KFJJ201114) and the Taishan Scholarship of Shandong Province.

References

1. T.A. Skotheim, J.R. Reynolds (Eds.), Handbook of Conducting Polymers, Theory, Synthesis, Properties and Characterization, third ed., CRC Press/Taylor & Francis Group, 2007.
2. R.J. Mortimer, A.L. Dyer, J.R. Reynolds, *Displays* 27 (2006) 2–18.
3. H. Tsuji, C. Mitsui, Y. Sato, E. Nakamura, *Adv. Mater.* 21 (2009) 3776–3779.
4. Q. Zhang, A. Cirpan, T.P. Russell, T. Emrick, *Macromolecules* 42 (2009) 1079–1082.
5. B. Bezgin, A. Cihaner, A.M. Önal, *Thin Solid Films* 516 (2008) 7329–7334.
6. A.J.C. da Silva, F.A.R. Nogueira, J. Tonholo, A.S. Ribe, *Sol. Energy Mater. Sol. Cells* 95(2011) 2255–2259.
7. N.M. Rowley, R.J. Mortimer, *Sci. Prog.* 85 (2002) 243–262.
8. P.M. Beaujuge, J.R. Reynolds, *Chem. Rev.* 110 (2010) 268–320.
9. S. Celebi, D. Baran, A. Balan, L. Toppare, *Electrochim. Acta* 55 (2010) 2373–2376.
10. E. Sahin, P. Camurlu, L. Toppare, V.M. Mercore, I. Cianga, Y. Yagci, *Polym. Int.* 54 (2005) 1599–1605.
11. M. Ak, M.S. Ak, G. Kurtay, M. Güllü, L. Toppare, *Solid State Sci.* 12 (2010) 1199–1204.
12. P. Berdyczko, W. Domagala, A. Czardybon, M. Lapkowski, *Synth. Met.* 159 (2009) 2240–2244.

13. J.R. Reynolds, J.P. Ruiz, A. D. Child, K. Nayak, D.S. Marynick, *Macromolecules* 24 (1991) 678–687.
14. J.G. Killian, Y. Gofer, H. Sarker, T.O. Poehler, P.C. Searson, *Chem. Mater.* 11 (1999) 1075–1082.
15. W.S. Schlindwein, Y. Gofer, H. Sarker, T.O. Poehler, P.C. Searson, *J. Electroanal. Chem.* 460 (1999) 46–52.
16. D.J. Irvin, J.R. Reynolds, *Polym. Adv. Technol.* 9 (1998) 260–265.
17. G. Sonmez, C.K.F. Shen, Y. Rubin, F. Wudl, *Angew. Chem. Int. Ed.* 43 (2004) 1498–1502.
18. L.Y. Xu, J.S. Zhao, C.S. Cui, R.M. Liu, J.F. Liu, H.S. Wang, *Electrochim. Acta* 56 (2011) 2815–2822.
19. G. Sonmez, H. Meng, F. Wudl, *Chem. Mater.* 16 (2004) 574–580.
20. S.C. Ng, L.G. Xu, H.S.O. Chan, *J. Mater. Sci. Lett.* 16 (1997) 1738–1740.
21. H. Sarker, Y. Gofer, J.G. Killian, T.O. Poehler, P.C. Searson, *Synth. Met.* 97 (1998) 1–6.
22. R.R. Yue, J.K. Xu, B.Y. Lu, C.C. Liu, Y.Z. Li, Z.J. Zhu, S. Chen, *J. Mater. Sci.* 44 (2009) 5909–5918.
23. G.W. Lu, G.Q. Shi, *J. Electroanal. Chem.* 586 (2006) 154–160.
24. K. Kham, S. Sadki, C. Chevrot, *Synth. Met.* 145 (2004) 135–140.
25. C. Pozo-Gonzalo, J.A. Pomposo, J.A. Alduncin, M. Salsamendi, A.I. Mikhaleva, L.B. Krivdin, B.A. Trofimov, *Electrochim. Acta* 52 (2007) 4784–4791.
26. W. Kaim, J. Fiedler, *Chem. Soc. Rev.* 38 (2009) 3373–3382.
27. D.M. de Leeuw, M.M.J. Simenon, A.R. Brown, R.E.F. Einerhand, *Synth. Met.* 87 (1997) 53–59.
28. Y.F. Li, Y. Cao, J. Gao, D.L. Wang, G. Yu, A.J. Heeger, *Synth. Met.* 99 (1999) 243–248.
29. J. Hwang, J.I. Son, Y.-B. Shim, *Sol. Energy Mater. Sol. Cells* 94 (2010) 1286–1292.
30. E. Yildiz, P. Camurlu, C. Tanyeli, I. Akhmedov, L. Toppare, *J. Electroanal. Chem.* 612 (2008) 247–256.
31. E. Sefer, F.B. Koyuncu, E. Oguzhan, S. Koyuncu, *J. Polym. Sci.: Part A: Polym. Chem.* 48 (2010) 4419–4427.
32. A.Cihaner, F. Algi, *Electrochim. Acta* 54 (2008) 786–792.
33. H.-M. Wang, S.-H. Hsiao, *J. Polym. Sci.: Part A: Polym. Chem.* 49 (2011) 337–351.
34. B. Yigitsoy, S. Varis, C. Tanyeli, I.M. Akhmedov, L. Toppare, *Electrochim. Acta* 52 (2007) 6561–6568.
35. U. Bulut, A. Cirpan, *Synth. Met.* 148 (2005) 65–69.